Vaccine 40 (2022) 6830–6838

Contents lists available at ScienceDirect

Vaccine

journal homepage: www.elsevier.com/locate/vaccine

Intranasal immunization with HRSV prefusion F protein and CpG adjuvant elicits robust protective effects in mice

Hu Ren [a,1], Hai Li [a,1], Lei Cao [a], Zhan Wang [a], Yangzi Zhou [a], Jinyuan Guo [a], Yan Zhang [a], Hongtu Liu [a,b,*], Wenbo Xu [a,b,*]

[a] NHC Key Laboratory of Medical Virology and Viral Diseases, National Institute for Viral Disease Control and Prevention, Chinese Center for Disease Control and Prevention, Beijing, China
[b] Center for Biosafety Mega-Science, Chinese Academy of Sciences, Wuhan, Hubei, China

ARTICLE INFO

Article history:
Received 8 June 2022
Received in revised form 9 August 2022
Accepted 23 September 2022
Available online 15 October 2022

Keywords:
Human respiratory syncytial virus
Intranasal immunization
CpG adjuvant
Protective effects

ABSTRACT

Human respiratory syncytial virus (HRSV) is a leading cause of lower respiratory tract infections in elderly individuals and young children/infants and can cause bronchiolitis and even death. There is no licensed HRSV vaccine. An ideal vaccine should induce high titers of neutralizing antibodies and a Th1-biased immune response. In this study, we used EXPI293 cells to express the fusion (F) protein with a prefusion conformation (PrF) and compared the safety and efficacy of intranasal immunization with PrF in combination with two mucosal adjuvants (CpG ODN and liposomes) in mice. After two intranasal administrations, mice in the PrF + CpG group produced high titers of neutralizing antibodies (4961) and a Th1-biased immune response compared with the PrF + Lipo group. The lung viral load of mice in the PrF + CpG group was significantly reduced (3.5 log) compared with that in the adjuvant control group, and the survival rate was 100 %, while the survival rate of mice in the PrF + Lipo group was only 67 %. At the same time, this immunization strategy reduced the pathological damage to the lungs in mice. In conclusion, the combination of PrF and CpG adjuvant is immunogenic, elicits a Th1 type immune response, and completely protects mice from a lethal HRSV challenge. It is worthy of further evaluation as an HRSV vaccine in clinical trials.

Clinical trial registration.

This study was not related to human participation or experimentation.

1. Introduction

Human respiratory syncytial virus (HRSV) is the leading cause of acute lower respiratory tract infection (ALRI) in infants and young children worldwide, as well as the major pathogen infecting the elderly and immunocompromised populations [1]. In 2015, 33.1 million HRSV-ALRIs occurred in children under 5 years of age worldwide, resulting in approximately 3.2 million hospitalizations and 59,600 hospitalized deaths. Of these, approximately 45 percent of HRSV-ALRI hospitalizations and in-hospital deaths occurred in children younger than six months of age [2]. In addition, in 2015, the number of hospitalizations for HRSV acute respiratory infection (ARI) in the elderly worldwide was estimated at 336,000, with approximately 14,000 hospitalized deaths [3]. Although mortality due to HRSV is lower in developed countries than in developing countries, the social and economic burdens associated with HRSV globally are quite high [4–5]. The global direct medical costs associated with inpatient and outpatient HRSV-ALRIs in young children were estimated to be approximately 4.82 billion EUR in 2017, with developing countries alone accounting for 3.13 billion EUR, placing a huge economic burden on health systems, governments and society [6].

Despite the high disease burden, there is still no licensed HRSV vaccine. The development of an effective HRSV vaccine faces many obstacles and challenges. In the 1960 s, the formaldehyde-inactivated HRSV vaccine (FI-HRSV) not only failed to prevent HRSV infection in infants and young children but also caused enhanced respiratory disease (ERD), with an infant hospitalization rate as high as 80 %, and eventually-two infants died, causing the development of the RSV vaccine to nearly stall [7]. To develop a safe vaccine, understanding the mechanisms that lead to ERD is

* Corresponding authors at: NHC Key Laboratory of Medical Virology and Viral Diseases, National Institute for Viral Disease Control and Prevention, Chinese Center for Disease Control and Prevention, Beijing, China.
E-mail addresses: liuht@ivdc.chinacdc.cn (H. Liu), wenbo_xu1@aliyun.com (W. Xu).
[1] These authors contributed equally to this article.

https://doi.org/10.1016/j.vaccine.2022.09.071
0264-410X/

critical. A widely accepted theory is that the increased severity of lung disease caused by FI-HRSV is due to low antibody neutralization capacity and an overactive Th2-biased immune response [8–9].

HRSV has three transmembrane glycoproteins: the highly glycosylated G protein, the F fusion protein, and the small hydrophobic SH protein. Among them, G protein and F protein are the only two protective antigens. The antigenic variability of G protein in the two subtypes of HRSV A and B is relatively large, while the F protein is highly conserved. The neutralizing antibodies induced by the F protein can inhibit the viral infection of the two subtypes with similar efficiency [10]. Therefore, the F protein has become the main target of neutralizing antibodies and vaccine development. During intracellular maturation, the HRSV F precursor (F0) is cleaved by the furin protease to generate disulfide-linked F1 and F2 fragments. When the virus fuses with the host cell membrane, the F protein changes from a prefusion conformation to a postfusion conformation. According to a previous study, the most potent neutralizing antibody recognized a neutralizing site present only in the prefusion F protein [11]. According to the Program for Appropriate Technology in Health (PATH) statistics, as of September 2021, 27 vaccine candidates were in different stages of clinical trials, three of which have entered Phase III, including two subunit vaccines and one adenovirus vector vaccine, all based on the prefusion F protein design [12].

It is one of the regulatory requirements to provide ERD survey data for vaccine candidates before entering clinical trials [13]. Therefore, in addition to enhancing neutralizing activity through structure-based approaches, a safe HRSV vaccine should simultaneously induce a Th1-biased cellular response. A previous report has also shown that promoting a balanced, HRSV-specific, Th1-biased immune response can clear viral infections without causing excessive or damaging inflammation in infected tissues [14]. A prefusion F vaccine formulated with alum (aluminum hydroxide) induces a Th2-biased immune response in mice that exacerbates airway eosinophilia and mucus accumulation when exposed to HRSV. In contrast, the prefusion F vaccine containing the Th1/Th2 balanced adjuvant Advax-SM not only inhibited HRSV replication but also prevented airway eosinophilia and mucus accumulation [15].

For viruses transmitted by the respiratory tract, intranasal immunization is considered attractive because it induces strong systemic and nasal mucosal immune responses [16] and robust tissue-resident memory CD8 T cells (TRMs), which act as the first line of defense against recurrent infection. It has been proven to have a special role in the prevention of HRSV disease [17–18]. Meanwhile, our previous study also showed that the intranasal immunization of F protein with CpG oligodeoxynucleotide (CpG ODN) adjuvant was superior to the intramuscular immunization for the induction of mucosal IgA antibodies or neutralizing antibodies [19].

However, intranasal immunization with HRSV F protein alone will not produce protective immunity, and therefore it must rely on safe and effective mucosal adjuvants to enhance the immune response [20]. Liposomes are closed annular sac-like structural bodies composed of lipids and cholesterol with low reactogenicity that are capable of carrying a variety of antigens, other adjuvants and/or functional molecules to further enhance the immune-enhancing effect or initiate an immune response of the Th1 and/or Th2 pathways, thereby establishing ideal immunity [21–22]. CpG ODN is a toll-like receptor 9 (TLR9) agonist that induces IL-12 production in antigen-presenting cells (APCs) and subsequently stimulates an antigen-specific Th1-mediated cellular immunity response involving cytotoxic T lymphocytes (CTLs) [23]. CpG ODN has been widely used as an adjuvant for various antiviral candidate vaccines, such as those against hepatitis C virus (HCV), human immunodeficiency virus (HIV) and hepatitis B virus (HBV) [24]. CpG ODN has also been used in the development of HRSV subunit intranasal vaccines and has been shown to elicit long-term mucosal and systemic immune responses, including memory CD8 T cells, with complete protection against HRSV challenge [25–26].

In this study, a prefusion F (PrF) vaccine formulated with CpG ODN elicited strong neutralizing antibodies and improved protective Th1-biased cellular immune responses compared with the PrF vaccine formulated with liposomes. When challenged with lethal HRSV doses, these immune responses enhanced resistance to viral replication, reduced lung pathology, and improved survival in mice. In conclusion, our study demonstrates that the combination of PrF with adjuvant CpG ODN is a safe and protective vaccine candidate that deserves further study.

2. Materials and methods

2.1. Protein expression and purification

The PrF glycoprotein sequence was derived from the HRSV A strain (GenBank: KY296733.1). To prevent the transformation of the structure after furin cleavage, amino acids 98 ∼ 144 of F (including the furin cleavage site, p27 peptide and part of the fusion peptide) were replaced with the flexible linker "GGGSGGGSGGGS". At the same time, to enhance the trimerization of the monomer, the C-terminal transmembrane segment (TM) and the intracellular segment were removed and replaced with a β-sheet conformation Foldon sequence (GYIPEAPRDGQAYVRKDGEWVLLSTFL) derived from T4 phage. To stabilize the prefusion form of F and maintain epitope Ø, 6 amino acids were mutated (S155C, S190F, V207L, S290C, D486C and D489C) [27]. To facilitate purification, a 6 × His tag and a Strep-tag II tag were added to the end of the protein. The nucleotide sequence was ligated into the expression vector pcDNA3.4 after codon optimization and transiently transfected into EXPI293 suspension cells (Thermo Fisher). Cell culture supernatants were collected on Day 3 after plasmid transfection and initially purified by Ni-Sepharose chromatography (GE Healthcare), followed by further protein purification on Strep-Tactin resin (GE Healthcare).

2.2. SDS–PAGE and western blotting

For SDS–PAGE, purified protein samples were treated with reducing agents in SDS buffer, heated at 95 ℃ for 5 min, and subjected to gel electrophoresis using a homemade gel. The gel was stained with rapid staining solution (Biodragon). For western blots, proteins in the gel were electrotransferred onto nitrocellulose membranes (GE Healthcare). The membrane was blocked with 10 % fetal bovine serum (FBS) for 1 h at room temperature. After washing, the membrane was incubated with palivizumab for 1 h at room temperature, washed, and then incubated with HRP-conjugated goat anti-human IgG secondary antibody (ZSGB-BIO) for 30 min at room temperature. After washing the membrane, detection was performed with a chemiluminescent reagent (Thermo Fisher).

2.3. Enzyme-linked immunosorbent assay (ELISA)

To assess antibody binding of purified PrF and postfusion F (Sino Biological), F protein was diluted to 0.5 μg/ml with phosphate buffered saline (PBS) in 96-well ELISA plates (Haimen Yingke) at 4 ℃ overnight and 100 μl was added to each well. Then, 10 % (v/v) FBS was added to PBS, followed by blocking at 37 ℃ for 2 h. The ELISA plates were washed with PBS containing 0.05 % (v/v) Tween 20 (PBST) and incubated with serial dilutions of 5C4 anti-

body (for epitope Ø, which is only present in prefusion F; gifted by Ningshao Xia from Xiamen University) or palivizumab (for epitope Ⅱ, which is present in both prefusion F and postfusion F) for 1 hr at 37 ℃. The ELISA plates were washed again and incubated with HRP-conjugated goat anti-mouse (5C4) or anti-human (palivizumab) IgG secondary antibody (ZSGB-BIO) for 1 h at 37 ℃. After washing the ELISA plates, the color was developed with 3,3′,5,5′-tetramethylbenzidine (TMB) substrate, the reaction was terminated with 2 M hydrochloric acid, and the absorbance was measured at 450 nm by a microplate reader.

To evaluate the titers of binding and subtype antibodies (IgG1 and IgG2a) against PrF protein in the sera of immunized mice, PrF protein was diluted to 0.5 μg/ml with PBS and coated overnight on ELISA plates at 4 ℃ and 100 μl was added to each well. The ELISA plates were blocked at 37 ℃ for 2 h and then washed three times with PBST. Mouse serum was serially diluted 4-fold (starting with a 1:50 dilution), transferred to the ELISA plates, and incubated at 37 ℃ for 1 h. After three washes with PBST, HRP-conjugated anti-mouse IgG, IgG1 and IgG2a secondary antibodies (ZSGB-BIO) were diluted 1:5000 and added to the ELISA plates for an additional 1 h incubation. The ELISA plates were washed again, TMB was added to develop color for 10 min, the reaction was stopped with 2 M hydrochloric acid, and the absorbance was measured at 450 nm by a microplate reader. Serum antibody titers (EC50) were determined by four-parameter curve fitting in GraphPad Prism 8.0.2 software. Background readings were subtracted from each well prior to curve fitting.

2.4. Negative staining

A total of 0.5 μl of purified PrF protein sample with a concentration of 0.02 mg/ml was added dropwise to the carbon-coated copper grid with a hydrophilization treatment, and after standing for 45 s, excess water was gently wiped off with filter paper. The copper grid was quickly cleaned with three drops of ultrapure water and three drops of 0.2 % (w/v) uranyl acetate. The copper grid was in contact with the last drop of 0.2 % (w/v) uranyl acetate for 45 s and blotted dry with filter paper. The samples were examined using a Talos L120C (accelerating voltage 120 kV) with a sample magnification of 57000 ×.

2.5. Vaccination and challenge

Female BALB/c mice (6–8 weeks) were purchased from Charles River Laboratories, Beijing, and randomly divided into seven groups as follows: (1) PrF, (2) PrF + neutral liposome (gifted from Maxvax) (PrF + Lipo), (3) PrF + CpG (Invivogen), (4) neutral liposome control, (5) CpG control, and (6) and (7) placebo groups (protein buffer). The protein dosage was 15 μg. Except for the seventh group (placebo/mock), which had 6 mice, the other groups had 15 mice. Nasal immunization was performed on Days 0 and 21 in a volume of 50 μl. Two weeks after the second immunization, all but the seventh group (placebo/mock) were challenged with the RSV/Long strain (1×10^6 PFU in 50 μl). Mice were lightly anesthetized with isoflurane for immunization and RSV challenge. At 4, 7 and 10 days post-challenge/infection (dpi), 5 mice in each group (2 in the placebo/mock) were sacrificed, and the lungs and spleens were removed. The left lung was perfused with 4 % paraformaldehyde for histopathological examination, while the right lung was weighed, homogenized and used for nucleic acid assessment. Spleens were analyzed by ELISpot. After the spleen was harvested, under sterile conditions, it was sheared, milled, and processed through a 70 μm cell strainer, and lymphocytes were isolated by adding lymphocyte separation medium. Serum samples were collected before the primary immunization and at 14, 34, 39 (4 dpi), 42 (7 dpi) and 45 (10 dpi) days after the primary immunization. All animal experiments complied with the requirements of the animal experiment ethics inspection of the Chinese Center for Disease Control and Prevention (No. 20210120001). The HRSV strain was preserved in the Department of Measles of the National Institute for Viral Disease Control and Prevention, Chinese Center for Disease Control and Prevention. This strain was obtained after long-term passage of the Long strain (ATCC, VR-26) in Hep-2 cells (ATCC, CCL-23).

2.6. HRSV neutralization assay

Mouse serum was treated at 56 ℃ for 30 min to inactivate complement. Starting at a 1:10 dilution, 4-fold serial dilutions of the serum samples in DMEM with 2 % FBS were prepared. Diluted serum was mixed 1:1 with the HRSV/Long strain (1500 PFU/ml) in a total volume of 100 μl. The mixture of virus and serum samples was incubated at 37 ℃ and 5 % CO_2 for 2 h. After incubation, the mixture was added to Hep-2 cells at a concentration of 3×10^5 cells per well for 1 h of adsorption. The viral fluid was discarded, the cells were covered with 1.2 % carboxymethylcellulose medium, and the plate was incubated in a 37 ℃ incubator. After 4 days, the overlay was removed, and the cells were fixed with 0.04 % crystal violet stain for 10 min, rinsed and air-dried. The number of plaques in each well was recorded, and serum neutralizing antibody titers (IC50) were determined by four-parameter curve fitting in GraphPad Prism 8.0.2 software. The HRSV/Long strain used for the neutralization assay and mouse challenge are the same stocks.

2.7. Elispot assays

The number of T cells secreting IFN-γ and IL-4 was determined by a mouse ELISpot kit (Mabtech). According to the manufacturer's instructions, the ELISA plates precoated with an anti-mouse IFN-γ or anti-IL-4 monoclonal antibody were washed with sterile PBS and then equilibrated with RPMI 1640 cell culture medium (Gibco) containing 10 % FBS. Mouse splenocytes (3×10^5 cells/well) were added to the plates. PrF protein (500 ng/well) was added to the wells for stimulation. Phytohemagglutinin (PHA) was added as a positive control. Unstimulated cells served as negative controls. After 42 h in culture, the cells were removed, and the plates were treated with biotinylated IFN-γ or IL-4 detection antibody, HRP-conjugated streptavidin and substrate. When the stain was strong enough to be observed, the plates were rinsed thoroughly with deionized water, and development was stopped. The number of spots was determined using an automated ELISpot reader and image analysis software.

2.8. Digital PCR

The right lung of the mouse was collected, weighed, homogenized, and centrifuged at 5000 rpm for 10 min, and 200 μl of the supernatant was added to the virus extraction kit (Tianlong Technology) to extract mouse lung nucleic acid. The primers and probe sequences of the HRSV N gene (upstream primer sequence: 5′AGATCAACTTCTGTCATCCAGCAA3′; downstream primer sequence: 5′ATTGATACTCCTAATTATGATGTGC3′; probe sequence: 5′CACCATCCAACGGAGCACAGGAGAT3′) were used to prepare the droplet generation amplification system. Analysis was performed with the Naica™ Crystal Microdroplet Digital PCR System.

2.9. Histopathological staining and statistical analysis

Lung tissue was treated with 4 % paraformaldehyde, paraffin-embedded and sectioned. Hematoxylin-eosin (HE) and periodic acid Schiff (PAS) staining and pathological description were

performed by the pathological sample preparation company. The histopathologist knew nothing about the experimental design. The HE-stained lung pathological films were scored according to the degree of inflammatory cell infiltration in different parts, and the scores were as follows: 0 (normal), 1 (mild inflammation), 2 (moderate inflammation), 3 (marked inflammation) and 4 (severe inflammation). The scoring indicators were the degree of alveolar wall thickening, interstitial pneumonia, alveolitis and bronchiolitis. The severity of each group was then assessed using the sum of the pathology scores.

All data were analyzed using GraphPad Prism version 8.0.2. Differences between groups were examined using one-way ANOVA (Tukey). Differences were considered significant if $P < 0.05$.

3. Results

3.1. PrF protein identification

The PrF protein contains 525 amino acids (Fig. 1A). SDS–PAGE and western blotting showed that the molecular weight was approximately 70 k_D (Fig. 1B), and the expression level was approximately 12.5 mg/L. Electron micrographs acquired by electron microscopy negative staining showed that PrF protein was in a lollipop-like trimer conformation with a length of approximately 14 nm (Fig. S1). The ELISA results showed that the PrF protein reacted with both the 5C4 antibody and palivizumab, while the postfusion F only reacted with palivizumab (Fig. 1C and D).

3.2. Intranasal immunization with PrF protein and CpG adjuvant induces a high-level antibody response in mice

To study the immunogenicity of PrF protein, BALB/c mice in each group were vaccinated with two doses of 15 μg PrF that was unadjuvanted or formulated into a liposome- or CpG-adjuvanted vaccine, with an interval of 21 days. Mice receiving placebo (adjuvant or protein buffer only) served as negative controls. Serum samples were collected at various time points after vaccination (Fig. 2A). The results showed that no matter whether it was after the first immunization (Day 14), after the second immunization (Day 34) or after the challenge (Day 39), the combined IgG antibody titers in the PrF + CpG group were significantly higher than those in the PrF + Lipo and PrF groups (Fig. 2B). In addition to inducing high titers of binding antibodies, the PrF + CpG group also showed induction of high levels of neutralizing antibodies. After the second immunization (Day 34), the geometric mean titer (GMT) of neutralizing antibody in the PrF + CpG group reached 3382 (IC50), while that in the PrF + Lipo group was 564 and that in the PrF group was 131. After the challenge (Day 39), the neutralizing antibody titers of the three groups decreased and then tended to rise, reaching the highest value within the study period at Day 45, with a GMT of 4961 in the PrF + CpG group and 3256 in the PrF + Lipo group (Fig. 2C).

3.3. Intranasal immunization with PrF protein and CpG adjuvant induces a Th1-biased immune response in mice

To determine the type of immune response induced, this study assessed PrF protein-specific IgG1 and IgG2a in serum. The levels of IgG1 and IgG2a and the ratio of the two (IgG2a/IgG1) in the PrF + CpG group were significantly higher than those in the PrF + Lipo and PrF groups before and after the HRSV challenge (Fig. 3A-C), and IgG2a/IgG1 gradually increased in the PrF + CpG group, indicating the induction of a more balanced Th1/Th2 response. To further determine the bias of the immune response, we examined the levels of IFN-γ and IL-4 secreted by PrF protein in restimulated splenocytes in vitro. Compared with that in the PrF + Lipo group, the number of IFN-γ-secreting cells was significantly higher in the PrF + CpG group (Fig. 3D), while the number of IL-4-secreting cells was lower (Fig. 3E). The PrF + CpG group had a higher ratio of IFN-γ- to IL-4-secreting cells, indicating the existence of a Th1 bias (Fig. 3F). However, for the PrF + Lipo group, there was no evidence of Th1 bias in either the IgG2a/IgG1 ratio or the ratio of IFN-γ-/IL-4-secreting cells.

3.4. Intranasal immunization with PrF protein and CpG adjuvant protects mice from a lethal dose viral challenge and prevents mice from losing weight.

To determine whether the PrF vaccine protects mice from HRSV infection, all but the seventh group (placebo/mock) were challenged with 1×10^6 PFU RSV/Long strain 14 days after boosting, and survival and body weight were monitored daily for 10 days after challenge. The results showed that the mice in the negative control group began to die on the second day after challenge, and most of the mice in the negative control and PrF protein groups died on the third day. The PrF protein immunization group had no protective effect on the mice. All died on the sixth day (Fig. 4A). In contrast, the survival rate of mice in the PrF + Lipo group was approximately 67 % and that in the PrF + CpG group was 100 %, indicating that PrF protein immunization with CpG adjuvant completely protected mice from lethal doses in a HRSV virus challenge.

All mice began to lose weight after HRSV challenge. Mice in the PrF + CpG group began to recover starting on the second day after challenge, and the mice in the PrF + Lipo group began to recover starting on the third day, while the weight of mice immunized only with adjuvant and protein buffer continued to decrease (Fig. 4B). On the second day after challenge, the weight loss of mice in the PrF + CpG group was significantly less than that in the PrF + Lipo group (Table S1). These results suggest that PrF protein immunization with CpG or liposome adjuvant is protective against HRSV challenge.

3.4. Intranasal immunization with PrF protein and CpG adjuvant reduces lung pathology and viral nucleic acid copy number

To investigate the safety of the vaccine, lung pathology in HRSV-infected mice was assessed by histochemical analysis. Lung tissue was harvested and stained with HE and PAS to assess lung histopathology at 4, 7 and 10 days after HRSV challenge. After HRSV infection, mice in the adjuvant control group exhibited severe inflammation, with parenchymal lesions in the lungs with diffuse hemorrhage (Fig. 5A). PAS results showed massive mucus secretion in the lungs (Fig. S2). The normal alveolar structure was almost invisible in the lungs of mice in the PrF group, the alveolar septa were significantly thickened, the capillaries were dilated, a large number of neutrophils were present in the alveolar interstitium, and a large amount of mucus was present in the alveolar cavity. In contrast, the pulmonary pathology of the PrF + Lipo group and PrF + CpG group was improved. The alveolar interstitium was dominated by lymphocytes and plasma cells, and the formation of lymphocyte nests and lymphoid nodules was observed locally. The lung pathological score decreased with increasing observation time, indicating that although the vaccine-immunized mice still showed a certain inflammatory response after challenge, vaccine immunization could alleviate the disease process after virus infection, and with increasing days, the lung pathology of the mice was further alleviated (Fig. 5B). However, compared with the PrF + CpG group, the pulmonary bronchial beaker cells in the PrF + Lipo group had significantly proliferated, and exudation and some inflammatory cells were observed in the alveolar cavity (Fig. S2).

In addition, lung tissue was harvested on Days 4, 7, and 10 postchallenge, and viral nucleic acid copy numbers were mea-

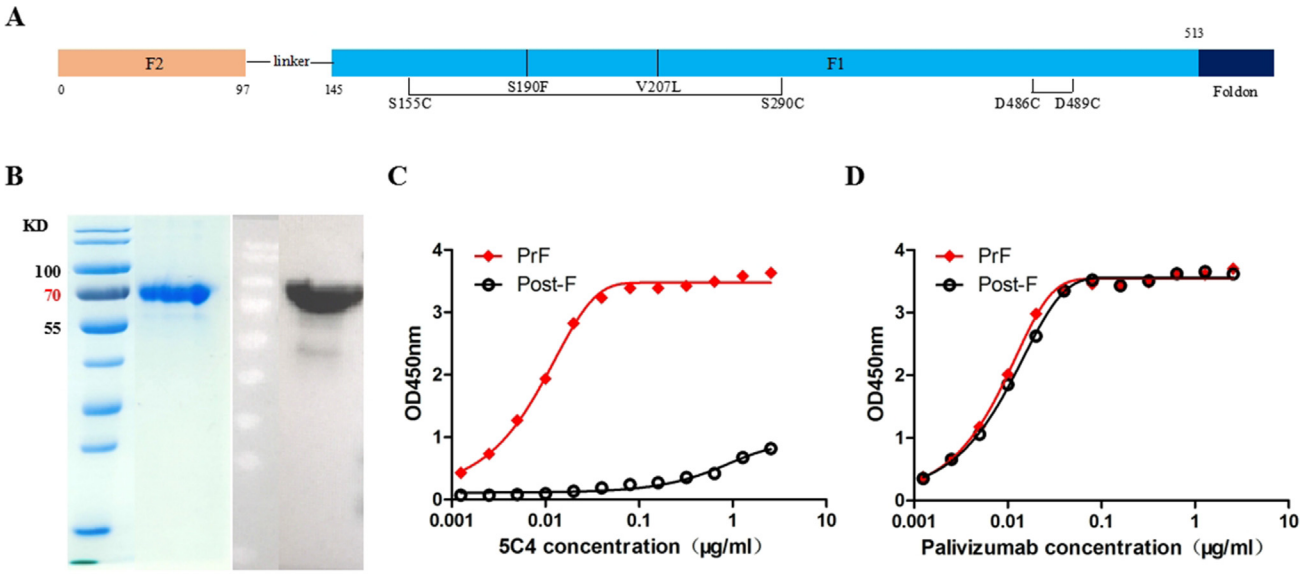

Fig. 1. Evaluation of PrF protein. (A) Schematic diagrams of HRSV PrF protein constructs. (B) Purified PrF protein was analyzed by SDS–PAGE (left panel) and western blotting (right panel). (C) PrF protein was assessed by ELISA for 5C4 antibody binding. (D) PrF protein was assessed by ELISA for palivizumab antibody binding.

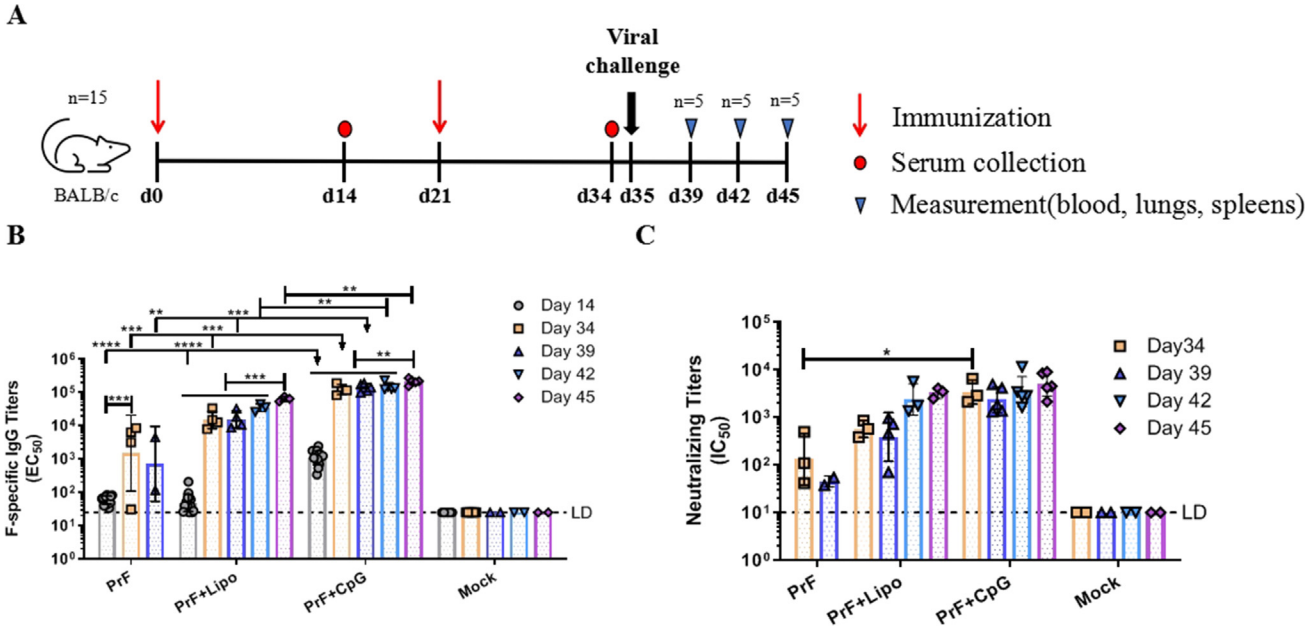

Fig. 2. Antibody responses to PrF protein in this study. (A) Time course of immunization, sampling, viral challenge and measurement. Mice were immunized intranasally (i.n.) with PrF protein or placebo and boosted with an equal dose of protein at Day 21 post-priming. Serum samples were collected as indicated. Mice were challenged i.n. with the HRSV/Long strain (1×10^6 PFU in 50 μl). Mock group was only immunized with protein buffer without challenge. Lungs and spleens were harvested at 4 days, 7 days and 10 days after challenge. (B) The ELISA results show serum IgG titers against the HRSV F protein. LD indicates the limit of detection, which is half of the lowest dilution of serum, and for this experiment, LD = 25. (C) The HRSV/Long strain neutralization assay results show the 50 % neutralization titer. LD is half of the lowest dilution of serum, and for this experiment, LD = 10. The data represent the geometric means ± SD. Statistically significant differences were measured by appropriate one-way ANOVA (*, $P < 0.05$; **, $P < 0.01$; ***, $P < 0.001$; ****, $P < 0.0001$).

sured. On Day 4 postchallenge, the highest viral load was detected in the adjuvant control group, and the PrF group was comparable to the adjuvant control group. Compared with the adjuvant control group and the PrF group, the average viral nucleic acid copy number in the PrF + Lipo group and PrF + CpG group was significantly reduced, with the PrF + Lipo group decreasing by 1.2 log and the PrF + CpG group decreasing by 3.5 log, which represents a very low level. On Day 7 postchallenge, 4 of the 5 mice in the PrF + CpG group had almost no nucleic acid detected in their lungs (Fig. 5C). These results are consistent with the results of the neutralizing antibody assessment. The higher the neutralizing antibody level was, the lower the number of viral nucleic acid copies in the lungs of the mice after challenge.

4. Discussion

Previous studies have demonstrated that higher neutralizing antibodies are associated with protection against infection and reduced viral replication, as well as protection against natural reinfection with HRSV [28–29]. In terms of neutralizing antibody pro-

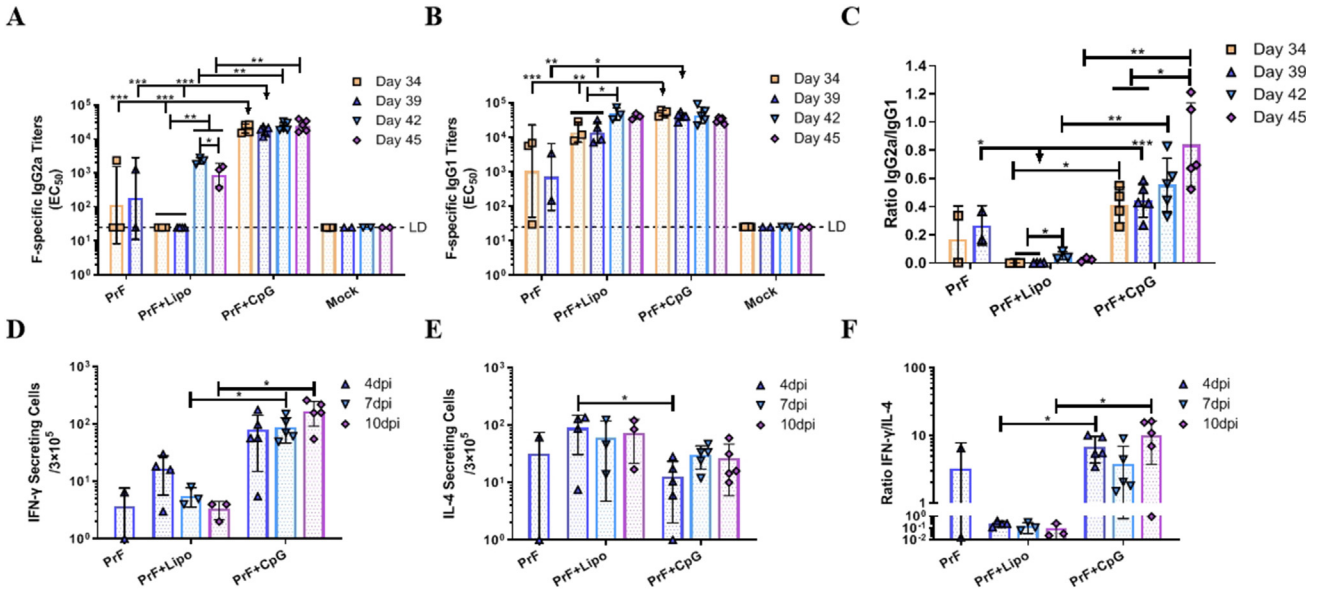

Fig. 3. Types of immune responses to PrF protein. Serum samples were harvested before and after challenge. Mock group was only immunized with protein buffer without challenge. PrF-specific IgG2a (A) and IgG1 (B) responses were determined by ELISA. The data represent the geometric means ± SD. LD indicates the limit of detection, which is half of the lowest dilution of serum, and for this experiment, LD = 25. (C) The ratio of IgG2a/IgG1. Spleen cells were harvested at 4 days, 7 days and 10 days after challenge, and splenic IFN-γ (D) and IL-4 (E) responses to PrF protein were determined by ELISpot. The data for the cytokine-secreting cells are expressed as the difference between the number of spots per 3×10^5 cells in PrF-stimulated wells and the number of spots per 3×10^5 cells in medium-treated wells. The data represent the means ± SD. (F) The ratio of IFN-γ-/IL-4-secreting cells. Statistically significant differences were measured by appropriate one-way ANOVA (*, P < 0.05; **, P < 0.01; ***, P < 0.001; ****, P < 0.0001). The horizontal black dashed line indicates the limit of detection, and dpi indicates the day post-infection.

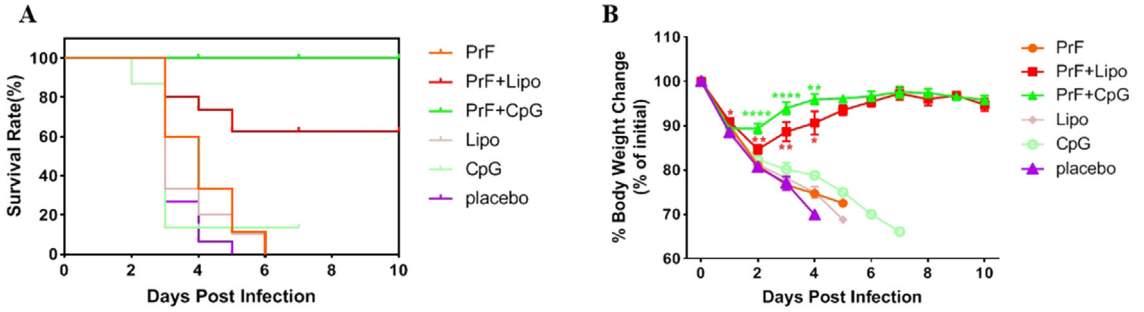

Fig. 4. Fourteen days after booster immunization, mice were challenged with 1×10^6 PFU of the high-passage HRSV/Long strain, and the survival rate and body weight were measured daily for 10 days after infection. (A) Survival curves of mice immunized with PrF protein with or without adjuvant after infection (15 mice per group). (B) The average relative body weight ± SEM of all mice in each group (compared with Day 0). Statistically significant differences were measured by appropriate one-way ANOVA (compared with placebo) (*, P < 0.05; **, P < 0.01; ***, P < 0.001; ****, P < 0.0001), and the color indicates the group.

duction, the titer of neutralizing antibody in rhesus monkeys immunized with prefusion F was 80 times higher than that induced by postfusion F [30]. Therefore, prefusion F was selected as the candidate antigen in this study. By modifying the protein to give it a stable prefusion conformation [27], the HRSV F antigen was prepared with a eukaryotic expression system, which expressed F had a prefusion trimer structure (Fig. 1C and D, S2).

Although candidate prefusion F antigens can generate neutralizing antibodies, low immunogenicity remains a problem, as evidenced by lower levels of HRSV F-specific and neutralizing antibodies in the F protein-immunized group (Fig. 2B). Therefore, prefusion F was formulated with liposomes or an CpG ODN adjuvant. Of these two formulations, the CpG ODN adjuvant outperformed the liposome adjuvant, producing higher neutralizing antibodies at all time points. In addition, the number of viral nucleic acid copies in the lungs of mice in the CpG ODN adjuvant group was also very low. After 4 days of challenge, the number of viral nucleic acid copies in the lungs was only $10^{2.2}$, which was significantly lower than that of the adjuvant control group ($10^{5.7}$) (Fig. 5C). More importantly, CpG ODN significantly enhanced Th1 immune responses in immunized mice, which was confirmed by the IgG2a/IgG1 ratio and ELISpot analysis (Fig. 3). Changes in the type of immune response may prevent ERD, as indicated by low viral nucleic acid copy numbers and rapid weight recovery from viral challenge (Fig. 4B). At the same time, CpG ODN completely prevented the death of the mice (Fig. 4A), and although liposomes could increase the production of neutralizing antibodies and significantly reduce the number of viral nucleic acid copies in the lungs, they produced a Th2-biased cellular immunity. After challenge, pulmonary bronchial beaker cells significantly proliferated, and mucus was secreted, which did not fully protect mice from lethal viral dose challenge. When administered subcutaneously or orally to mice, smaller lipid vesicles (<150 nm) have been reported to promote the development of Th2 responses, whereas larger lipid vesicles (>200 nm) promote IFN-γ and typical Th1 responses [31–32]; the liposomes used in this study were approximately 120 nm and therefore may be more biased toward Th2 responses.

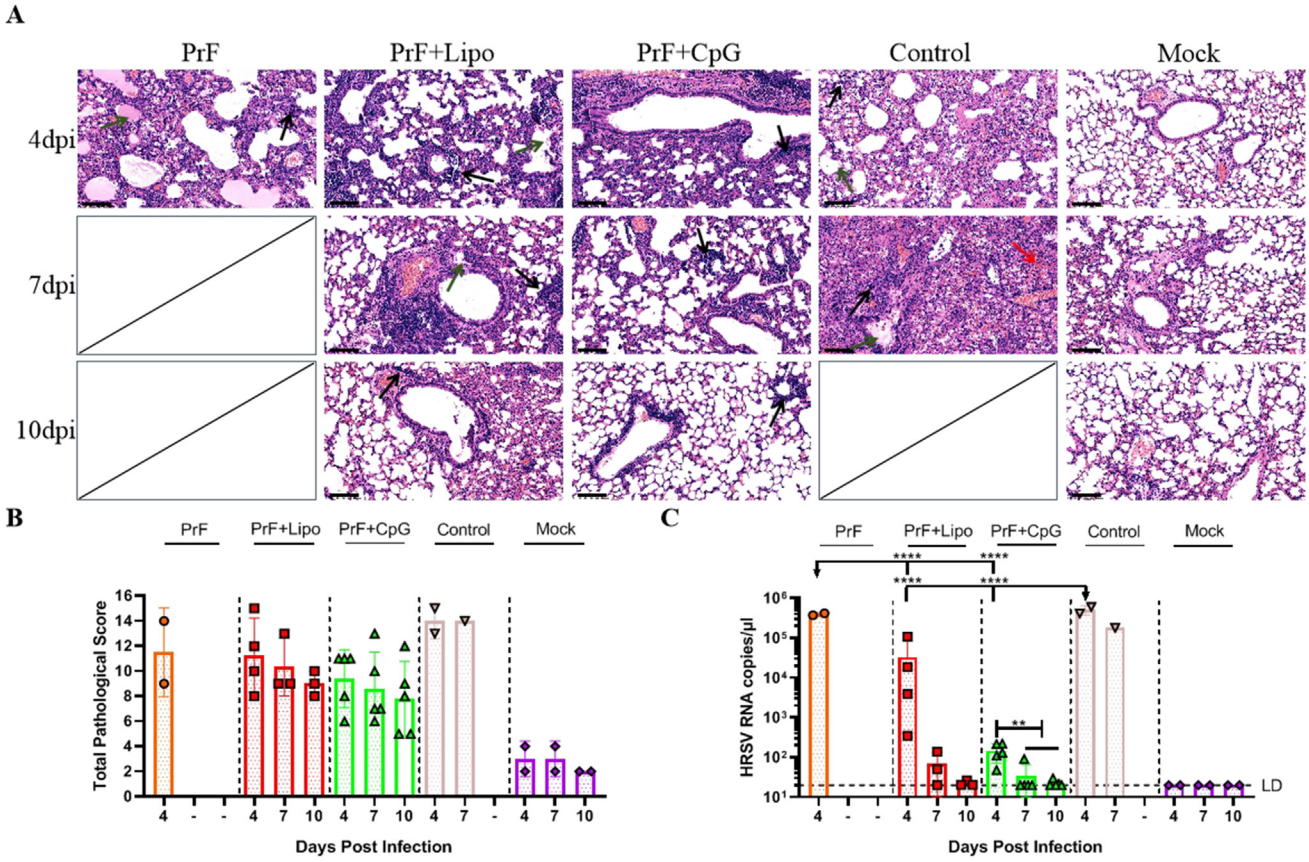

Fig. 5. Histopathological analysis of PrF-immunized mice challenged with HRSV/Long strain. Mock group was only immunized with protein buffer without challenge. (A) Representative mouse lungs stained with HE at 20 × magnification are shown. Lung tissue infiltration of inflammatory cells (black arrow), local bleeding (red arrow) and exudation of eosinophilic serous material in the alveolar cavity (green arrow) are marked. The blank indicates that all the mice in that group had died by these time points. Scale bar (black line): 100 μm. (B) Pulmonary pathology scores were calculated according to the criteria listed in the histopathology section. The data show the means ± SD of the scores calculated from all mice in each group. (C) Pulmonary viral nucleic acid copy number in lung tissue of immunized mice at 4 days, 7 days and 10 days after challenge. The results are shown as the means ± SD of viral nucleic acid copy number calculated from all mice in each group. According to the instructions, LD = 20. Statistically significant differences were measured by appropriate one-way ANOVA (*, $P < 0.05$; **, $P < 0.01$; ***, $P < 0.001$; ****, $P < 0.0001$). The control group was the liposome and CpG adjuvant control. The horizontal black dashed line indicates the limit of detection, and dpi indicates the day post-infection. (For interpretation of the references to color in this figure legend, the reader is referred to the web version of this article.)

Animal models of HRSV infection are useful for understanding disease pathogenesis and evaluating treatments. Nonhuman primates (NHPs), cotton rats, mice, sheep, Syrian hamsters, chinchillas, guinea pigs, and ferrets have all been used to study HRSV [33]. Of these, chimpanzees are the only animal species that are naturally susceptible to HRSV infection [34]. However, research using chimpanzees for new vaccines and antiviral treatments is limited due to the high cost of animal care, and therefore most such experiments are performed on rodents, especially mice. To better and more intuitively evaluate the protective effect of the vaccine, the mouse lethal model was selected in this study. This model was previously established in our laboratory. The HRSV/Long strain (ATCCVR-26) was serially passaged on Hep-2 cells 50 times, and the mortality rate of mice after lethal dose challenge was 100 % [35]. With this model, it was observed that immunization of CpG ODN with prefusion F can completely prevent the death of mice, which presumably may be related to the high neutralizing antibodies and/or Th1-biased immune response, because the liposome adjuvant group, with a relatively low neutralizing antibody and Th2-biased immune response, could not completely prevent the death of mice. This is consistent with the two generally recognized absolute protective indicators and meets the review requirements for candidate vaccine evaluation, proving the applicability of this lethal model to the preclinical protective evaluation of HRSV vaccine candidates. The effect of the lower limit of protective antibody titer and Th2 bias on lethality in mice needs to be explored in further experiments. In general, the establishment of the lethal model facilitates the rapid screening of a large number of candidate vaccines, which will further promote the research enthusiasm for HRSV vaccines and is worthy of further research. At present, our laboratory has found that the HRSV/Long strain has 7 amino acid mutations through full-length sequencing, and the next step will be to study the key virulence sites.

In humans, TLR9 is only expressed in plasmacytoid dendritic cells (PDCs) and B cells. However, in mice, in addition to the above cell types, TLR9 is also expressed in macrophages and myeloid dendritic cells (MDCs) [36–37]. This may affect the translation of CpG ODN from preclinical studies to clinical trials. However, CpG ODN has been shown to enhance immune responses in combination with vaccines in human clinical trials for the prevention of influenza, malaria, and hepatitis B [38–40]. At least three classes of CpG ODN have been identified based on their backbone, sequence, and immunostimulatory properties: class A (type D), class B (type K), and class C. CpG-A ODN activates PDCs to produce interferon-α (IFN-α) but cannot induce B-cell activation [41–42]. In contrast, CpG-B ODN strongly induces interleukin-6 (IL-6) production by B cells but promotes PDC maturation in the absence of IFN-α secretion [41,43]. Finally, CpG-C ODN combines the characteristics of class A and class B to activate PDCs and B cells [44]. The CpG ODN used in this study was class C, but almost all CpG ODNs used

in clinical trials are class B, and class A is occasionally used. Only class C has not been clinically tested. Whether it can play the role of activating PDCs and B cells in the human body requires further study. At the same time, it is worth noting that studies have shown that animals immunized with F protein purified from virus culture and CpG ODN combined intranasally have enhanced lung pathology after virus challenge [45], which may be related to the purity of F protein and the sequence of CpG ODN, because the use of eukaryotic system to express purified F protein and commercial CpG ODN of different sequences combined intranasally immunized mice did not find enhanced lung pathology after challenge [25], nor was it found in this study.

Currently, HRSV vaccines are designed mainly for three groups of people, including infants, pregnant women, and the elderly. Our vaccine design is mainly based on these three populations. This study has demonstrated the effect of prefusion F and CpG ODN adjuvant with intranasal immunization of adult mice. In the future, we will be to conduct research on young mice, pregnant mice and old mice, to preliminarily explore the immune response of prefusion F and CpG ODN adjuvant in mice with different immune states, in order to provide animal evidence for the clinical application of vaccines. At the same time, considering that most people have pre-existing antibodies, we plan to challenge and then immunize mice later to explore the impact of pre-existing antibodies on vaccine immunity.

This study has some limitations. First, this study should add non-lethal HRSV intranasal immunization and FI-HRSV intramuscular immunization in mice to compare the magnitude of antibody responses and cytokine responses to Th1 or Th2 type responses. Future studies will include these comparison groups. Second, the present study explored IFN-γ and IL-4 responses in splenocytes in mice after challenge, reflecting a combination of vaccine induced responses and infection induced early responses, and it is difficult to determine the Th1 versus Th2 bias of vaccine induced immunity. In the future, we will directly explore the Th1 and Th2 bias after vaccine immunization. Third, the adjuvant and protein used in this study are fixed doses, which may not be the best compatibility, we will explore the best dose in future studies. In general, our study shows that the combination of prefusion F and CpG ODN adjuvant enhances the production of neutralizing antibodies, improves the Th1-biased cellular immune response, and completely protects mice from lethal dose viral challenge. It is worthy of further evaluation as an HRSV vaccine in clinical trials.

Data availability

Data will be made available on request.

Declaration of Competing Interest

The authors declare that they have no known competing financial interests or personal relationships that could have appeared to influence the work reported in this paper.

Acknowledgments

We thank Professor Ningshao Xia (Xiamen University, Xiamen, China) for generously supplying the 5C4 antibody.

Funding

This work was supported by the Key Technologies R&D Program of the National Ministry of Science (2018ZX10713002 and 2018ZX10713001-003).

Role of the funding source

none.

Author contributions

HR, HL, LC, ZW, YZ, WBX and HTL designed the study and prepared the manuscript. HR, YZZ and JYG expressed and purified the protein. HR, HL and YZZ performed animal experiments and analyzed the data. All authors read and approved the final manuscript.

Additional information

Informed consent

This study was not related to human participation or experimentation.

Animal welfare

All the disposals were in accordance with the guideline of animal ethics from the Animal Experimental Ethical Committee of the Nation Institute for Viral Disease Control and Prevention.

Availability of materials

The data and materials used to support the findings of this study are available from the corresponding author upon request.

Appendix A. Supplementary data

Supplementary data to this article can be found online at https://doi.org/10.1016/j.vaccine.2022.09.071.

References

[1] Chatterjee A, Mavunda K, Krilov LR. Current state of respiratory syncytial virus disease and managemen. Infect Dis Ther 2021;10:5–16.
[2] Shi T, McAllister DA, O'Brien KL, Simoes EAF, Madhi SA, Gessner BD, et al. Global, regional, and national disease burden estimates of acute lower respiratory infections due to respiratory syncytial virus in young children in 2015: a systematic review and modelling study. Lancet 2017;390:946–58.
[3] Shi T, Denouel A, Tietjen AK, Campbell I, Moran E, Li X, et al. Global disease burden estimates of respiratory syncytial virus-associated acute respiratory infection in older adults in 2015: a systematic review and meta-analysis. J Infect Dis 2020;222:S577–83.
[4] Griffiths C, Drews SJ, Marchant DJ. Respiratory syncytial virus: infection, detection, and new options for prevention and treatment. Clin Microbiol Rev 2017;30:277–319.
[5] Haber N. Respiratory syncytial virus infection in elderly adults. Med Mal Infect 2018;48(6):377–82.
[6] Zhang SS, Akmar LZ, Bailey F, Rath BA, Alchikh M, Schweiger B, et al. Cost of respiratory syncytial virus-associated acute lower respiratory infection management in young children at the regional and global level: a systematic review and meta-analysis. J Infect Dis 2020;222(Supplement 7):S680–7.
[7] Kim HW, Canchola JG, Brandt CD, Pyles G, Chanock RM, Jensen K, et al. Respiratory syncytial virus disease in infants despite prior administration of antigenic inactivated vaccine. Am J Epidemiol 1969;89(4):422–34.
[8] Widjaja I, Wicht O, Luytjes W, Leenhouts K, Rottier PJM, van Kuppeveld FJM, et al. Characterization of epitope-specific anti-respiratory syncytial virus (anti-RSV) antibody responses after natural infection and after vaccination with formalin-inactivated RSV. J Virol 2016;90(13):5965–77.
[9] Graham BS, Henderson GS, Tang YW, Lu X, Neuzil KM, Colley DG. Priming immunization determines T helper cytokine mRNA expression patterns in lungs of mice challenged with respiratory syncytial virus. J Immunol 1993;151(4):2032–40.
[10] Empey KM, Peebles Jr RS, Kolls JK. Pharmacologic advances in the treatment and prevention of respiratory syncytial virus. Clin Infect Dis 2010;50(9):1258–67.
[11] Graham BS, Modjarrad K, McLellan JS. Novel antigens for RSV vaccines. Curr Opin Immunol 2015;35:30–8.
[12] Program for Appropriate Technology in Health. RSV Vaccine and mAb Snapshot, https://www.path.org/resources/rsv-vaccine-and-mab-snapshot/;2021 [accessed 28 September 2021].
[13] Higgins D, Trujillo C, Keech C. Advances in RSV vaccine research and development - A global agenda. Vaccine 2016;34(26):2870–3285.
[14] Bueno SM, González PA, Cautivo KM, Mora JE, Leiva ED, Tobar HE, et al. Protective T cell immunity against respiratory syncytial virus is efficiently induced by recombinant BCG. Proc Natl Acad Sci U S A 2008;105(52):20822–7.
[15] Eichinger KM, Kosanovich JL, Gidwani SV, Zomback A, Lipp MA, Perkins TN, et al. Prefusion RSV F immunization elicits Th2-mediated lung pathology in mice when formulated with a Th2 (but not a Th1/Th2-balanced) adjuvant despite complete viral protection. Front Immunol 2020;11:1673.
[16] Yang K, Varga SM. Mucosal vaccines against respiratory syncytial virus. Curr Opin Virol 2014;6:78–84.
[17] Morabito KM, Ruckwardt TR, Redwood AJ, Moin SM, Price DA, Graham BS. Intranasal administration of RSV antigen-expressing MCMV elicits robust tissue-resident effector and effector memory CD8+ T cells in the lung. Mucosal Immunol 2017;10(2):545–54.

[18] Jozwik A, Habibi MS, Paras A, Zhu J, Guvenel A, Dhariwal J, et al. RSV-specific airway resident memory CD8+ T cells and differential disease severity after experimental human infection. Nat Commun 2015;6:10224.
[19] Li H, Ren H, Cao L, Guo J, Zhang Y, Fang Q, et al. Comparison of the efficacy and safety of different immunization routes induced by human respiratory syncytial virus F protein with CpG adjuvant in mice. Biochem Biophys Res Commun 2022;618:54–60.
[20] Garg R, Latimer L, Simko E, Gerdts V, Potter A. van Drunen Littel-van den Hurk S. Induction of mucosal immunity and protection by intranasal immunization with a respiratory syncytial virus subunit vaccine formulation. J Gen Virol 2014;95(Pt 2):301–6.
[21] Wang T, Zhen Y, Ma X, Wei B, Wang N. Phospholipid bilayer-coated aluminum nanoparticles as an effective vaccine adjuvant-delivery system. ACS Appl Mater Interfaces 2015;7(12):6391–6.
[22] Wang N, Zhen Y, Jin Y, Wang X, Li N, Jiang S, et al. Combining different types of multifunctional liposomes loaded with ammonium bicarbonate to fabricate microneedle arrays as a vaginal mucosal vaccine adjuvant-dual delivery system (VADDS). J Control Release 2017;246:12–29.
[23] Klinman DM, Currie D, Gursel I, Verthelyi D. Use of CpG oligodeoxynucleotides as immune adjuvants. Immunol Rev 2004;199:201–16.
[24] Zhao H, Han Q, Yang A, Wang Y, Wang G, Lin A, et al. CpG-C ODN M362 as an immunoadjuvant for HBV therapeutic vaccine reverses the systemic tolerance against HBV. Int J Biol Sci 2022;18(1):154–65.
[25] Garlapati S, Garg R, Brownlie R, Latimer L, Simko E, Hancock RE, et al. Enhanced immune responses and protection by vaccination with respiratory syncytial virus fusion protein formulated with CpG oligodeoxynucleotide and innate defense regulator peptide in polyphosphazene microparticles. Vaccine 2012;30(35):5206–14.
[26] Garg R, Latimer L, Gerdts V, Potter A, van Drunen Littel-van den Hurk S. Vaccination with the RSV fusion protein formulated with a combination adjuvant induces long-lasting protective immunity. J Gen Virol 2014;95(Pt 5):1043-54.
[27] Zhang L, Durr E, Galli JD, Cosmi S, Cejas PJ, Luo B, et al. Design and characterization of a fusion glycoprotein vaccine for respiratory syncytial virus with improved stability. Vaccine 2018;36(52):8119–30.
[28] Bagga B, Cehelsky JE, Vaishnaw A, Wilkinson T, Meyers R, Harrison LM, et al. Effect of preexisting serum and mucosal antibody on experimental respiratory syncytial virus (RSV) challenge and infection of adults. J Infect Dis 2015;212(11):1719–25.
[29] Walsh EE, Falsey AR. Humoral and mucosal immunity in protection from natural respiratory syncytial virus infection in adults. J Infect Dis 2004;190(2):373–8.
[30] McLellan JS, Chen M, Joyce MG, Sastry M, Stewart-Jones GB, Yang Y, et al. Structure-based design of a fusion glycoprotein vaccine for respiratory syncytial virus. Science 2013;342(6158):592–8.
[31] Brewer JM, Tetley L, Richmond J, Liew FY, Alexander J. Lipid vesicle size determines the Th1 or Th2 response to entrapped antigen. J Immunol 1998;161(8):4000–7.
[32] Mann JF, Shakir E, Carter KC, Mullen AB, Alexander J, Ferro VA. Lipid vesicle size of an oral influenza vaccine delivery vehicle influences the Th1/Th2 bias in the immune response and protection against infection. Vaccine 2009;27(27):3643–9.
[33] Taylor G. Animal models of respiratory syncytial virus infection. Vaccine 2017;35(3):469–80.
[34] Altamirano-Lagos MJ, Díaz FE, Mansilla MA, Rivera-Pérez D, Soto D, McGill JL, et al. Current animal models for understanding the pathology caused by the respiratory syncytial virus. Front Microbiol 2019;10:873.
[35] Li H, Ren H, Cao L, Guo J, Song J, Zhang Y, et al. Establishment and application of a lethal model of an HRSV-Long variant strain in BALB/c mice. Exp Anim 2022.
[36] Hornung V, Rothenfusser S, Britsch S, Krug A, Jahrsdörfer B, Giese T, et al. Quantitative expression of toll-like receptor 1–10 mRNA in cellular subsets of human peripheral blood mononuclear cells and sensitivity to CpG oligodeoxynucleotides. J Immunol 2002;168(9):4531–7.
[37] Krug A, Towarowski A, Britsch S, Rothenfusser S, Hornung V, Bals R, et al. Toll-like receptor expression reveals CpG DNA as a unique microbial stimulus for plasmacytoid dendritic cells which synergizes with CD40 ligand to induce high amounts of IL-12. Eur J Immunol 2001;31(10):3026–37.
[38] Cooper CL, Davis HL, Morris ML, Efler SM, Krieg AM, Li Y, et al. Safety and immunogenicity of CPG 7909 injection as an adjuvant to Fluarix influenza vaccine. Vaccine 2004;22(23–24):3136–43.
[39] Sagara I, Ellis RD, Dicko A, Niambele MB, Kamate B, Guindo O, et al. A randomized and controlled Phase 1 study of the safety and immunogenicity of the AMA1-C1/Alhydrogel + CPG 7909 vaccine for Plasmodium falciparum malaria in semi-immune Malian adults. Vaccine 2009;27(52):7292–8.
[40] Cooper CL, Angel JB, Seguin I, Davis HL, Cameron DW. CPG 7909 adjuvant plus hepatitis B virus vaccination in HIV-infected adults achieves long-term seroprotection for up to 5 years. Clin Infect Dis 2008;46(8):1310–4.
[41] Aillot L, Bonnin M, Ait-Goughoulte M, Bendriss-Vermare N, Maadadi S, Dimier L, et al. Interaction between toll-like receptor 9-CpG oligodeoxynucleotides and hepatitis B virus virions leads to entry inhibition in hepatocytes and reduction of alpha interferon production by plasmacytoid dendritic cells. Antimicrob Agents Chemother 2018;62(4):e01741–817.
[42] Krug A, Rothenfusser S, Hornung V, Jahrsdörfer B, Blackwell S, Ballas ZK, et al. Identification of CpG oligonucleotide sequences with high induction of IFN-alpha/beta in plasmacytoid dendritic cells. Eur J Immunol 2001;31(7):2154–63.
[43] Hartmann G, Krieg AM. Mechanism and function of a newly identified CpG DNA motif in human primary B cells. J Immunol 2000;164(2):944–53.
[44] Hartmann G, Battiany J, Poeck H, Wagner M, Kerkmann M, Lubenow N, et al. Rational design of new CpG oligonucleotides that combine B cell activation with high IFN-alpha induction in plasmacytoid dendritic cells. Eur J Immunol 2003;33(6):1633–41.
[45] Prince GA, Mond JJ, Porter DD, Yim KC, Lan SJ, Klinman DM. Immunoprotective activity and safety of a respiratory syncytial virus vaccine: mucosal delivery of fusion glycoprotein with a CpG oligodeoxynucleotide adjuvant. J Virol 2003;77(24):13156–60.